

Electronic Supplementary Information

Broadband Ultrafast Photovoltaic Detectors Based on Large-scale Topological Insulator Sb₂Te₃/STO Heterostructures

Honghui Sun^{1,†}, Tian Jiang^{*1,2,3,5,†}, Yunyi Zang^{3,†}, Xin Zheng^{1,5}, Yan Gong³, Yong Yan⁴, Zhongjie Xu^{2,5}, Yu Liu², Liang Fang^{*1,5}, Xiang'ai Cheng^{2,5} and Ke He³

¹State Key Laboratory of High Performance Computing, College of Computer, National University of Defense Technology, Changsha 410073, China

²College of Optoelectronic Science and Engineering, National University of Defense Technology, Changsha 410073, China

³State Key Laboratory of Low-Dimensional Quantum Physics, Department of Physics, Tsinghua University, Beijing 100084, China

⁴Henan key laboratory of photovoltaic materials, college of physics and materials science, Henan Normal University, Xinxiang 453007, china

⁵Interdisciplinary Center of Quantum Information, National University of Defense Technology, Changsha 410073, China

Address correspondence to Tian Jiang, tjiang@nudt.edu.cn; Liang Fang,

lfang@nudt.edu.cn

1. Film thickness of Sb_2Te_3

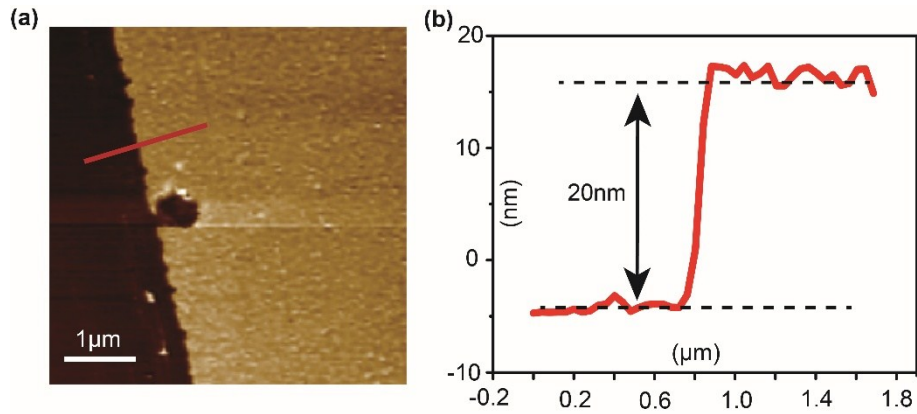


Figure S1. Film thickness of the Sb_2Te_3 film in $\text{Sb}_2\text{Te}_3/\text{STO}$ heterostructure. (a) The AFM image of 20 QL Sb_2Te_3 film. (b) The line profile along the red line in (a).

2. Absorption spectra of Sb_2Te_3 film

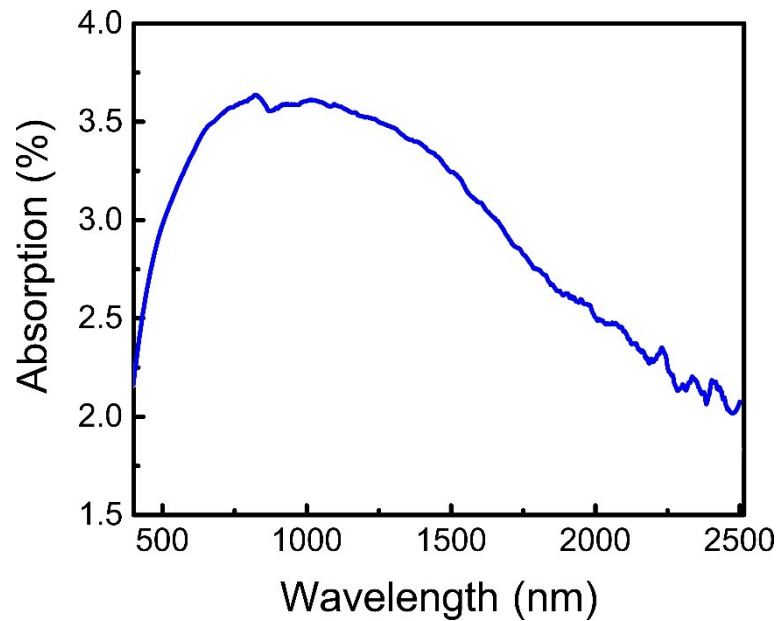


Figure S2. Absorption spectra of the Sb_2Te_3 topological insulation film with the thickness of 20 nm from 400 nm to 2500 nm.

3. Transmittance spectra of ITO top electrode

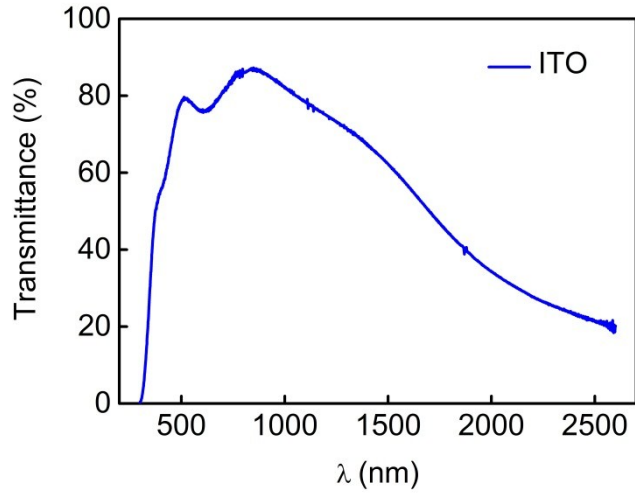


Figure S3. The transmittance spectra of the ITO top electrode.

4. Confirmation of the p-n junction in the $\text{Sb}_2\text{Te}_3/\text{STO}$ photodetector

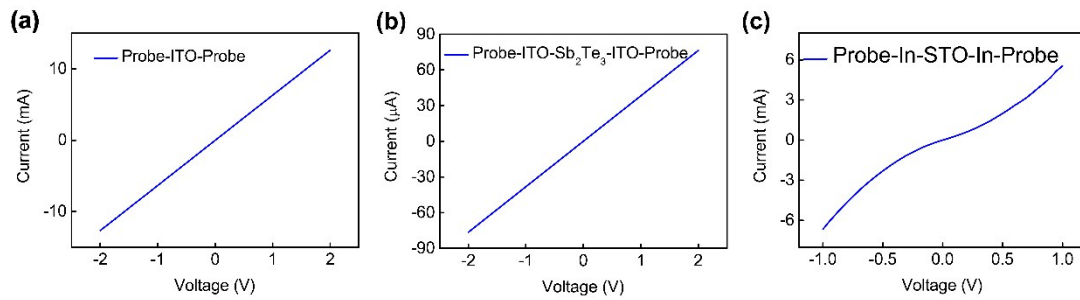


Figure S4. Contact performance. (a) and (b) show the contact behaviors of ITO with probe and Sb_2Te_3 , indicating perfect Ohmic contact. (b) ITO with Sb_2Te_3 contact, suggesting a negligible barrier.

5. Ideality factor.

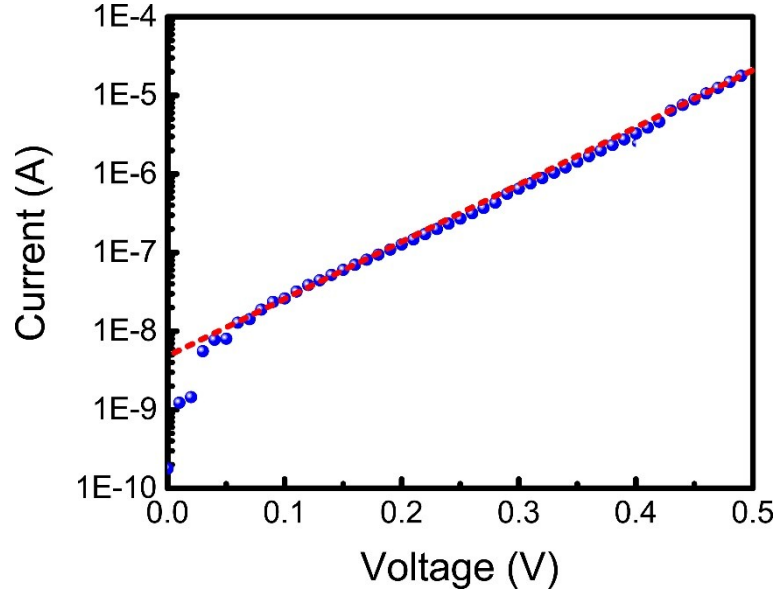


Figure S5. I-V curve of the Sb₂Te₃/STO heterostructure. The semi-logarithmic curve is fitted by a straight line.

The ideality factor (n) of the heterojunction could be deduced to be 1.59 from the slope of the semi-log I - V curve in the forward bias direction, according to the following equation:¹

$$n = \frac{q}{k_B T} \frac{dV}{d \ln I}$$

where q is the electron charge, k_B is the Boltzmann constant, and T is the absolute temperature.

6. Responsivity spectra from 405 nm to 1550 nm

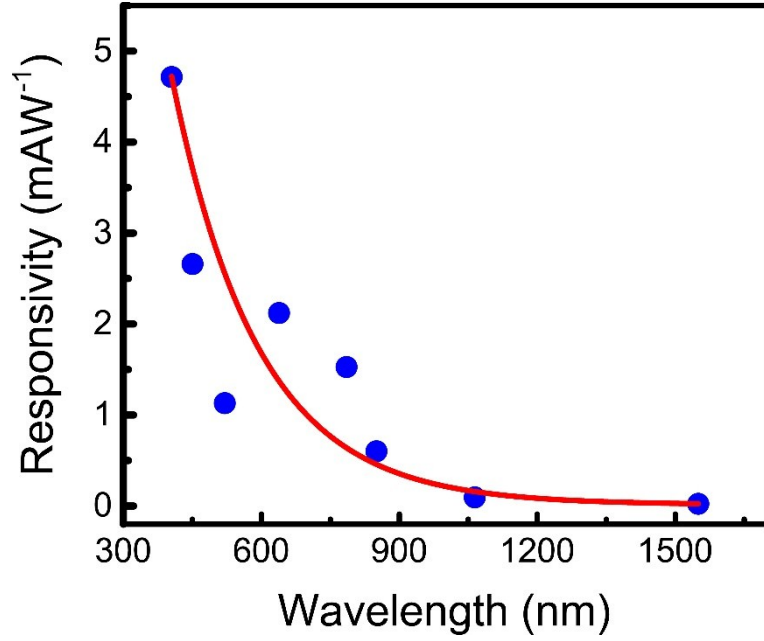


Figure S6. Responsivity spectra of the $\text{Sb}_2\text{Te}_3/\text{STO}$ photodetector. Power densities at each illumination wavelength were calibrated to be same (236.81mWcm^{-2}).

7. Hall effect measurement of STO at 300K

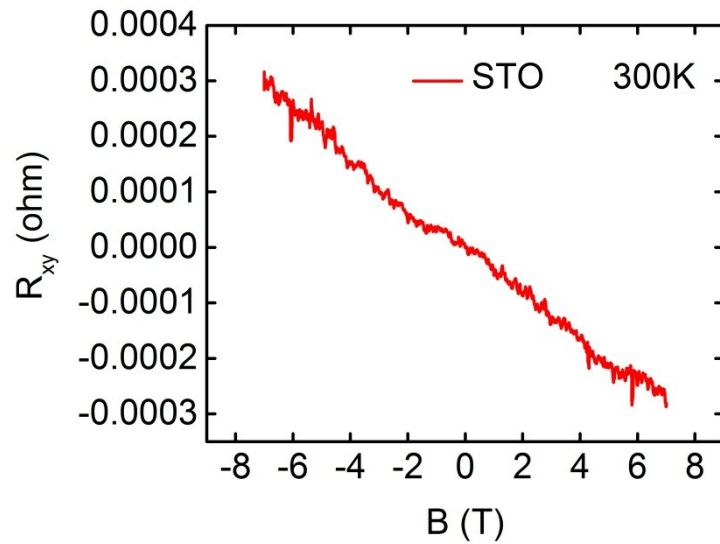


Figure S7. Hall effect measurement of STO at 300K. The electron concentration (N_e) of $3 \times 10^{20}\text{ cm}^{-3}$ is extracted from the Hall slop.

8. Temperature-dependent photoresponse of the heterostructure under 1064 nm illumination

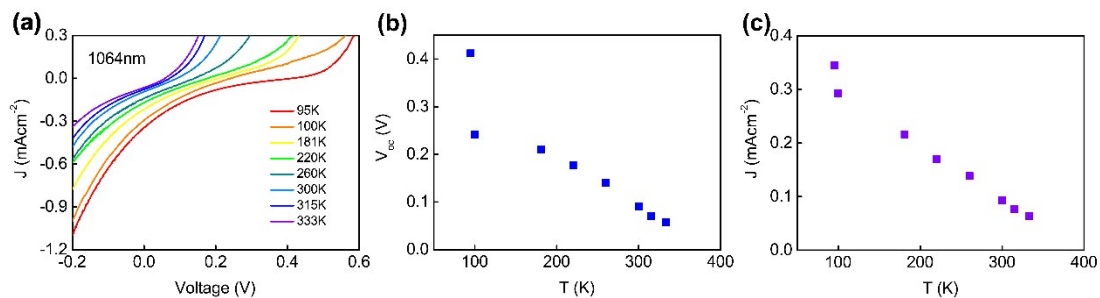


Figure S8. Temperature-dependent photoresponse of the heterostructure under 1064 nm illumination. (a) J-V characteristics of the heterostructure at different T. (b) and (c) show the dependence of V_{oc} and J_{sc} on temperature (T).

References:

1. X. Zhang, X. Zhang, X. Zhang, Y. Zhang, L. Bian, Y. Wu, C. Xie, Y. Han, Y. Wang and P. Gao, *Journal of Materials Chemistry*, 2012, **22**, 22873-22880.